# Incompressible Streamwise Flow Along an Unbounded Corner

K. N. Ghia*
*University of Cincinnati, Cincinnati, Ohio*

**The unbounded streamwise flow along a corner is analyzed based on the method of singular perturbations and matched asymptotic expansions. In view of the algebraic decay of the corner layer flow variables, the far-field boundary was placed at true infinity. Suitable transformations were used for the independent, as well as the dependent variables of the problem, to maintain the accuracy of the numerical solutions in the infinite computational domain. The detailed flow structure has been determined from the numerical solutions obtained by an alternating direction implicit scheme. The results are compared with earlier finite corner region solutions obtained by using higher-order asymptotic solutions to provide the far-field boundary conditions. The streamwise velocity shows good agreement. The secondary velocity shows some differences; possible reasons causing these differences are clearly explained.**

## I. Introduction

THE basic features of an important class of aerodynamics problems can be studied by analyzing the problem of streamwise flow along a corner formed by the intersection of two semi-infinite plates. Among such applications related to the study of the corner flow are wing-body junctions, wing-fin assemblies, the roots and tips of blades in turbomachinery, the walls of a wind tunnel, and air-breathing engine inlets. Although many of these applications require the knowledge of high-speed flow along internal corners formed by more complicated shapes as compared to flat plates, the basic axial corner formed by the intersection of two flat plates at 90° merits a thorough analysis, even for incompressible flow, as it possesses several features similar to the more general case. A detailed analysis revealing the flow structure of this basic case would provide understanding and insight about the corresponding high-speed corner flow studies.

Although attempts had been made earlier to analyze the corner flow problem, it was Rubin[1] who systematically and correctly formulated the problem using the method of matched asymptotic expansions similar to the scheme used by Stewartson[2] in his study of the quarter-infinite plate problem. A meaningful solution of the problem required the analytical determination of the corner flow asymptotic behavior. Pal and Rubin[3] formally demonstrated that all corner layer flow variables exhibit algebraic decay into the boundary layer away from the corner. Moreover, the cross flow velocities decay algebrically into the outer potential flow. Only the streamwise velocity and vorticity decay exponentially from the corner layer to the potential flow. This asymptotic analysis made it possible to determine the proper farfield boundary condition and obtain a numerical solution for a limited region of the corner flow problem.[4] Further, Tokuda[5] provided the detailed flow structure of the inner corner region by determining a Stokes slow-flow solution and an inertial-flow solution, properly matched in the region of overlap of the two solutions.

Ghia and Davis[6] analyzed the compressible corner flow problem following Rubin,[1] and presented an optimized solution for the incompressible corner flow problem for a finite region using an alternating direction implicit (ADI) method. The ADI method made it possible to determine accurate and rapidly converging solutions, and also showed good promise for obtaining stable solutions for larger regions of the corner layer. This is important because the asymptotic analysis needed for generating the proper far-field boundary condition for a finite region is very laborious and not straightforward for more practical corner configurations. In view of the algebraic behavior of the flow variables, it becomes necessary to determine some higher-order asymptotic solutions, depending on the location of the far-field boundary. On the other hand, the finite difference solution of a problem in an infinite domain involves two major difficulties, namely, 1) representation of an infinite region for the discretized problem by a reasonable number of grid points, and 2) satisfaction of boundary conditions at infinity. Therefore, a suitable formulation of the problem must be developed such that the asymptotic solution of the problem, at true infinity, can be obtained as a limiting solution. This would circumvent the need for determining higher-order asymptotic solutions of the problem.

Presented as Paper 74-559 at the AIAA 7th Fluid and Plasma Dynamics Conference, Palo Alto, Calif., June 17-19, 1974; submitted August 20, 1974; revision received January 20, 1975. This research was supported by ARL under Contract F33615-73-C-4014. The author is thankful to U. Ghia, R.T. Davis, and S.G. Rubin for their many useful suggestions and discussions, and to A. G. Mikhail for assistance in preparing the contour plots.

Index categories: Boundary Layers and Convective Heat Transfer—Laminar; Jets, Wakes, and Viscid-Inviscid Flow Interactions.

*Associate Professor Department of Aerospace Engineering. Member AIAA.

## II. Analysis

The corner flow geometry has been depicted in Fig. 1. The salient feature of this configuration is the infinite lateral curvature at the corner which introduces a geometrical singularity in the flowfield. The flowfield is inherently 3-D in character because of the viscous interaction of the boundary layers that develop on the two plates forming the corner.

Rubin and coworkers have made important contributions to the understanding of such boundary-region type of flows by presenting solutions for this important class of problems where 3-D boundary layer theory fails to yield the solution. The various regions delineated in Fig. 1 are identified as a potential flow, two boundary-layer flow regions on the plates at $y=0$ and $z=0$, and the flow in region IV is the "corner layer" where the gradients in both the $y$ and $z$ directions are large compared to $x$-direction gradients. Also, the absence of a length scale in the problem leads to the existence of streamwise similarity far downstream from the leading edge when no streamwise pressure gradient is present.

### Mathematical Formulation

The lowest-order corner layer equations have been derived in Refs. 4 and 6 in terms of the dependent variables $u$, $\phi$, $\psi$, and $\theta$, using the similarity coordinates $(\eta,\zeta)$ where

$$\eta=y\,Re^{1/2}/(2x)^{1/2},\ \zeta=z\,Re^{1/2}/(2x)^{1/2}$$
$$\phi=\eta u-v,\ \psi=\zeta u-w,\ \theta=\psi_\eta-\phi_\zeta \qquad (1)$$

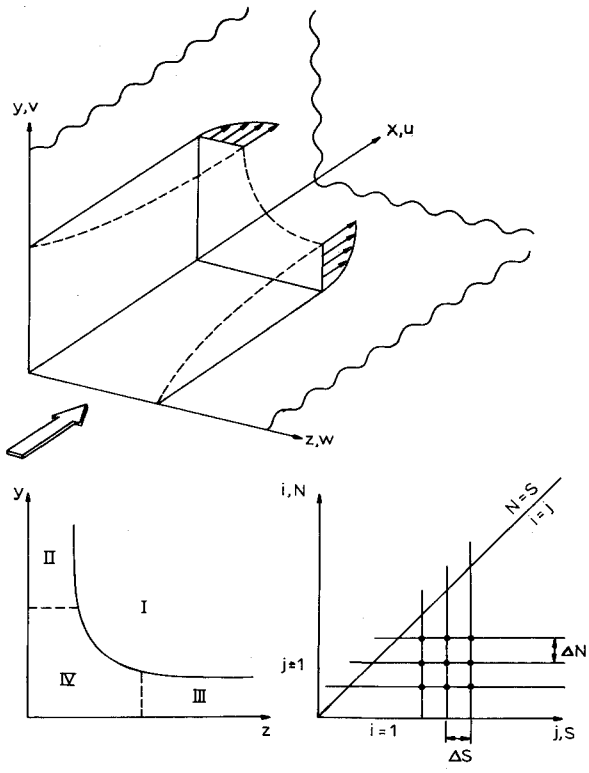


**Fig. 1 Corner flow configuration and discretized grid system.**

and $Re$ is the Reynolds number based on the freestream conditions and some reference length $L$. These equations are as follows.

Streamwise Momentum Equation:

$$u_{\eta\eta}+u_{\zeta\zeta}+\phi\, u_{\eta}+\psi\, u_{\zeta}=0 \tag{2}$$

Equation for $\phi$:

$$\phi_{\eta\eta}+\phi_{\zeta\zeta}+\theta_{\zeta}-2u_{\eta}=0 \tag{3}$$

Equation for $\psi$:

$$\psi_{\eta\eta}+\psi_{\zeta\zeta}-\theta_{\eta}-2u_{\zeta}=0 \tag{4}$$

Modified Streamwise Vorticity Equation:

$$\theta_{\eta\eta}+\theta_{\zeta\zeta}+\phi\theta_{\eta}+\psi\theta_{\zeta}+2u\theta+2\eta uu_{\zeta}-2\zeta uu_{\eta}=0 \tag{5}$$

Equations (3) and (4) for $\phi$ and $\psi$, respectively, were obtained by appropriately differentiating and combining the continuity equation and the definition of $\theta$, both of which were first-order differential equations in $\phi$ and $\psi$. Their conversion to Poisson-type second-order differential equations was found essential to the success of the ensuing numerical calculations.

Equations (2-5) are a set of coupled nonlinear elliptic partial differential equations and represent the starting point of the present analysis. They require boundary conditions to be specified on a closed boundary. The conditions at the wall boundary and at the symmetry boundary are straightfoward and will be discussed only after the flow equations have been written in their final form. The far-field boundary, when imposed at $\zeta\to\infty$, required careful treatment and is discussed next.

#### Asymptotic Boundary Conditions as $\zeta\to\infty$

The limiting equations at the far-field boundary can be obtained by taking the proper asymptotic limit, as $\zeta\to\infty$, of the governing differential equations. This requires knowledge of whether, or not, the flow variables of the problem become unbounded as $\zeta\to\infty$. For variables that are unbounded at $\zeta\to\infty$, it is also necessary to determine the manner in which they approach their unbounded asymptotic values; however, detailed knowledge of the higher-order asymptotic solutions is not required. For the present problem, this information is easily extracted from the asymptotic analysis of Pal and Rubin.[3] It can be shown that, as $\zeta\to\infty$, $\psi$ and $\theta$ grow linearly with $\zeta$. When used in Eqs. (2-5), this leads to the following limiting equations, as $\zeta\to\infty$.

$$u_{\infty_{\eta\eta}}+\phi_{\infty}\, u_{\infty_{\eta}}=o \tag{6}$$

$$\phi_{\infty_{\eta\eta}}-u_{\infty_{\eta}}=0 \tag{7}$$

$$\psi_{\infty_{\eta\eta}}-\theta_{\infty_{\eta}}=0 \tag{8}$$

$$\theta_{\infty_{\eta\eta}}+\phi_{\infty}\,\theta_{\infty_{\eta}}+2u_{\infty}\theta_{\infty}-\zeta u_{\infty}u_{\infty_{\eta}}=0 \tag{9}$$

where the subscript $\infty$ denotes quantities for $\zeta\to\infty$. These limiting equations may be recognized as the familiar equations for two-dimensional flow over a semi-infinite flat plate, with a cross-flow superimposed over it. Their solution will provide the necessary boundary condition at $\zeta\to\infty$.

It is observed in the previous formulation that the independent variables as well as some of the dependent variables become unbounded within the region of computation. This can lead to severe inaccuracies in the numerical calculations. Therefore, new variables must be defined through suitable transformations, such that all transformed quantities remain bounded everywhere in the computational domain.

#### Transformed Independent and Dependent Variables

The transformation of the independent variables is considered first. The mapping function sought must exhibit certain characteristic features in order to ensure accuracy of the numerical solution. 1) An infinite region must be transformed to a suitable finite region so as to allow the image points to be concentrated where the gradients are maximum. 2) The boundary conditions at infinity may be imposed directly as opposed to being satisfied asymptotically. 3) The stretching function is relatively simple to apply, has an explicit inverse relation and does not introduce any singularity in the flowfield.

A transformation of the independent variable that is based on the asymptotic behavior of the most slowly decaying dependent variable of the problem, usually proves to be the most suitable transformation. Accordingly, for the present problem, the transformed independent variables are defined as

$$N=\eta/(C+\eta) \qquad S=\zeta/(C+\zeta) \tag{10}$$

where the constant $C$ was selected so as to provide sufficient resolution in the viscous region. Use of the same transformation for both coordinates serves to preserve the symmetry of the problem. These transformations map the quarter-infinite $(\eta,\zeta)$ plane of the corner flow into a finite region such that $0\le N,\ S\le 1$. Moreover, $N_{\eta}$ and $N_{\eta\eta}$ vanish as $\eta\to\infty$. Therefore, as long as the transformed derivative $\partial/\partial N$ remains bounded as $\eta\to\infty$, then $\partial/\partial\eta\to 0$ as $\eta\to\infty$. This is also true for the $\zeta-S$ transformation. This demonstrates that the transformation possesses the asymptotic behavior of the flow variables built into itself. Sills[7] has discussed the merits of many such algebraic transformations.

The criteria considered essential in selecting suitable dependent variable transformations may be summarized as follows. 1) Unboundedness in the flow variables should be properly removed and, as far as possible, all the variables should be of about the same order of magnitude. 2) If possible, the algebraic decay of the flow variables must be removed.

Taking these requirements into consideration, new dependent variables are defined for the unbounded corner problem as

$$\bar{u}(\eta,\zeta)=u(\eta,\zeta) \tag{11a}$$

$$\bar{\phi}(\eta,\zeta)=\phi(\eta,\zeta)-\eta u(\infty,\zeta) \tag{11b}$$

$$\bar{\psi}(\eta,\zeta)=\psi(\eta,\zeta)-\zeta u(\eta,\infty) \tag{11c}$$

$$\bar{\theta}(\eta,\zeta)=\theta(\eta,\zeta)-\zeta u_{\eta}(\eta,\infty)+\eta u_{\zeta}(\infty,\zeta) \tag{11d}$$

With these transformations for the independent and the dependent variables, the problem will now be formulated in the $(N,S)$ plane.

**Governing Differential Equations in the Transformed $(N-S)$ Plane**

Streamwise Momentum Equation:

$$\bar{u}_{NN}N_{\eta}^2+\bar{u}_{SS}S_{\zeta}^2+[N_{\eta\eta}+\{\bar{\phi}+\eta\bar{u}(1,S)\}N_{\eta}]\bar{u}_N+[S_{\zeta\zeta}+\{\bar{\psi}+\zeta\bar{u}(N,1)\}S_{\zeta}]\bar{u}_S=0 \tag{12}$$

Equation for $\bar{\phi}$:

$$\bar{\phi}_{NN}N_{\eta}^2+\bar{\phi}_{SS}S_{\zeta}^2+\bar{\phi}_N N_{\eta\eta}+\bar{\phi}_S S_{\zeta\zeta}-2\bar{u}_N N_{\eta}+\bar{\theta}_S S_{\zeta}+\bar{u}_N(N,1)N_{\eta}=0 \tag{13}$$

Equation for $\bar{\psi}$:

$$\bar{\psi}_{NN}N_{\eta}^2+\bar{\psi}_{SS}S_{\zeta}^2+\bar{\psi}_N N_{\eta\eta}+\bar{\psi}_S S_{\zeta\zeta}-2\bar{u}_S S_{\zeta}-\bar{\theta}_N N_{\eta}+\bar{u}_S(1,S)S_{\zeta}=0 \tag{14}$$

Modified Streamwise Vorticity Equation:

$$\begin{aligned}\bar{\theta}_{NN}N_{\eta}^2+\bar{\theta}_{SS}S_{\zeta}^2+[N_{\eta\eta}+\{\bar{\phi}+\eta\bar{u}(1,S)\}N_{\eta}]\bar{\theta}_N\\+2\bar{u}\bar{\theta}+[S_{\zeta\zeta}+\{\bar{\psi}+\zeta\bar{u}(N,1)\}S_{\zeta}]\bar{\theta}_S\\-\bar{\phi}\bar{u}_S(1,S)S_{\zeta}+\bar{\psi}\bar{u}_N(N,1)N_{\eta}\\+\zeta[\{\bar{u}_{NN}(N,1)N_{\eta}^2+\bar{u}_N(N,1)N_{\eta\eta}\}\\\times\{\bar{\phi}-\bar{\phi}(N,1)+\eta\bar{u}(1,S)-\eta\}\\+2\bar{u}\,\bar{u}_N(N,1)N_{\eta}-2\bar{u}\,\bar{u}_N N_{\eta}]\\-\eta[\{\bar{u}_{SS}(1,S)S_{\zeta}^2+\bar{u}_S(1,S)S_{\zeta\zeta}\}\\\times\{\bar{\psi}-\bar{\psi}(1,S)+\zeta\bar{u}(N,1)-\zeta\}\\+2\bar{u}\,\bar{u}_S(1,S)S_{\zeta}-2\bar{u}\,\bar{u}_S S_{\zeta}]=0\end{aligned} \tag{15}$$

It is important to observe the particular form in which the transformed vorticity equation (15) has been arranged. The direct transformation of Eq. (5), using Eqs. (10) and (11), would lead to the appearance of the terms $\bar{u}_{NNN}(N,1)$ and $\bar{u}_{SSS}(1,S)$ in the transformed equation. These third-derivative terms have been replaced by their equivalent expressions obtained from the differentiated forms of the asymptotic momentum equation as $S\to 1$ and as $N\to 1$ (i.e., as $\zeta\to\infty$ and as $\eta\to\infty$ respectively). Moreover, it must be noted that, even though $\eta$ and $\zeta$ appear explicitly in Eq. (15), the equation is arranged such that these are multiplied by expressions that approach zero more rapidly than $1/\eta$ and $1/\zeta$, respectively, so that the products vanish in the limit as $\eta\to\infty$ and $\zeta\to\infty$. These points are particularly emphasized here because they constituted an essential step in the success of the present solution for the infinite computational domain.

Boundary Conditions:

The boundary conditions for the transformed problem are as follows. At the plate surface, i.e., $N=0$,

$$\bar{u}(0,S)=0,\ \bar{\phi}(0,S)=0,\ \bar{\psi}(0,S)=0,\ \bar{\theta}(0,S)=\bar{\psi}_N(0,S)N_{\eta}(0) \tag{16}$$

At the symmetry line, i.e., at $N=S$,

$$\bar{u}_N(N,N)=\bar{u}_S(N,N),\ \bar{\phi}_N(N,N)=\bar{\psi}_S(N,N),\ \bar{\psi}(N,N)=\bar{\phi}(N,N),\ \bar{\theta}(N,N)=0 \tag{17}$$

Equations for Asymptotic Boundary Condition at $S=1$:

The limiting equations appropriately transform to the following.

$$\bar{u}_{NN}(N,1)N_{\eta}^2+\bar{u}_N(N,1)N_{\eta\eta}+[\bar{\phi}(N,1)+\eta]\bar{u}_N(N,1)N_{\eta}=0 \tag{18}$$

$$\bar{\phi}_{NN}(N,1)N_{\eta}^2+\bar{\phi}_N(N,1)N_{\eta\eta}-\bar{u}_N(N,1)N_{\eta}=0 \tag{19}$$

$$\bar{\psi}_{NN}(N,1)N_{\eta}^2+\bar{\psi}_N(N,1)N_{\eta\eta}-\bar{\theta}_N(N,1)N_{\eta}=0 \tag{20}$$

$$\bar{\theta}_{NN}(N,1)N_{\eta}^2+[N_{\eta\eta}+(\bar{\phi}(N,1)+\eta)N_{\eta}]\bar{\theta}_N(N,1)+2\bar{u}(N,1)\bar{\theta}(N,1)+\bar{\psi}(N,1)\bar{u}_N(N,1)N_{\eta}=0 \tag{21}$$

Boundary Conditions for Asymptotic Equations:

The boundary conditions for the previous limiting equations are as follows. At the plate surface, i.e., at $N=0$,

$$\bar{u}(0,1)=0,\ \bar{\phi}(0,1)=0,\ \bar{\psi}(0,1)=0,\ \bar{\theta}(0,1)=\bar{\psi}_N(0,1)N_{\eta}(0) \tag{22}$$

At the symmetry line, i.e., at $N=1$,

$$\bar{u}_N(1,1)=0,\ \bar{\phi}_N(1,1)=0,\ \bar{\psi}(1,1)=\bar{\phi}(1,1),\ \bar{\theta}(1,1)=0 \tag{23}$$

The mathematical formulation of the problem is now complete. The numerical analysis used is described briefly in the next section; the results obtained are discussed in detail.

## III. Results and Discussion

The ADI method is proving to be a very efficient method for the numerical solution of parabolic-elliptic partial differential equations. A two-step ADI scheme is employed in the present work also to obtain numerical solutions of the elliptic equations governing the unbounded corner flow. To this end, a fictitious time-derivative term is introduced in each of the governing differential equations (12-15). Second-order accurate central differences are used for all spatial derivatives, while simple backward differences are used for the temporal derivatives. The time levels of the various terms in the equations are chosen so as to obtain a totally second-order accurate numerical scheme. The sequence in which the equations are solved during each iteration is chosen such that second-order accuracy of the scheme can be achieved wihout resorting to unnecessary internal iterations.

The flow in the corner is governed by a system of equations and boundary conditions from which all parameters have been removed by employing suitable nondimensionalizations and similarity transformations. Nevertheless, the discretized formulation of the problem, for the purpose of numerical

solution, introduces certain parameters into the problem, e.g., the spatial and the temporal step sizes used in the finite difference formulas. In addition, for the present problem, the manner of treating certain boundary conditions and the location of the far-field boundary may also represent parameters of the numerical solution. Since the differential problem must not depend on these parameters, it is important to select these parameters such that they have minimal influence on the numerical solution. To aid in this selection, as well as to provide a check for the programing details, the computer program was first used to determine the solution in a finite region of the corner by placing the far-field boundary at some values of $S$ less than unity, to correspond to a finite value of $\zeta_{max}$. The asymptotic formulae of Pal and Rubin,[3] suitably transformed, would provide the boundary conditions at this $\zeta_{max}$. Good agreement with the earlier finite corner results of Refs. 4 and 6 would then indicate that the finite difference method has been correctly implemented.

Therefore, results were first obtained for a case with $\zeta_{max} = 12.857$. A grid of $(51 \times 51)$ points in the transformed plane for $0 \leq N, S \leq 1$ was found, after some experimentation, to provide reasonable accuracy and resolution. This led to $S = 0.72$ corresponding to $\zeta_{max} = 12.857$, so the solution was obtained in one triangular half of a region of $(37 \times 37)$ points. Some typical results are presented in Figs. 2 and 3, plotted in terms of the untransformed variables in order to provide direct comparison with earlier finite corner studies.[4,6] Good agreement is obtained for the quantities $u$, $\phi$, $\psi$, and $\theta$. The cross flow velocities $v$ and $w$ are not in complete agreement. However, there are some distinct differences in the present procedure as compared to the earlier one, e.g., the grid spacing in terms of $\eta$ and $\zeta$, and also the variables used in the formulation. The position of $\zeta_{max}$ was also seen earlier to affect the cross flow to a small extent. The differences seen in Fig. 3 are small enough to be attributed to these factors.

Computations were then made for the infinite corner region. The optimum starting time steps for the infinite corner problem were found to be 0.05, 1.0, 0.05, and 1.0 for the $\bar{u}$, $\bar{\phi}$, $\bar{\theta}$, and $\bar{\psi}$ equations, respectively. These were reduced, as calculations progressed, for the first 200 iterations. With these optimization procedures, the method converged in 262 iterations, requiring 10 min of computing time for an IBM 370/165 computer. The solution was said to have converged when the cross-flow velocity functions $\bar{\phi}$ and $\bar{\psi}$ differed by no more than 1% over the two sweeps of ADI scheme. As in the solution of the limiting far-field equations (18-21), the converged solution for the infinite corner was also obtained after requiring $\bar{\theta}$ to vanish for $\eta$, $\zeta \geq 15.0$, a condition well satisfied by the exponential decay of $\bar{\theta}$ from the viscous region into the potential flow region.

Typical results are presented in Figs. 4 and 5. The earlier results of the finite corner problem are also included in these figures. The present results are seen to reproduce the finite corner results, in the inner region, for the streamwise velocity $\bar{u}$ and surface vorticity function $\bar{\theta}_{wall}$. The results for the cross flow velocity compare well in general trend, but differ by a maximum of about 10% near the peak value occurring at $\eta = \zeta \simeq 4.0$. Several definite reasons may be cited as responsible for these differences. The value of $\zeta_{max}$ was seen to influence the cross flow velocity in the finite region solution. Therefore, it is obvious that the results obtained with finite $\zeta_{max}$ and truncated asymptotic boundary values should differ, to some extent, from those obtained with $\zeta_{max} \to \infty$. In view of the algebraic asymptotic behavior of the solution, it should be more accurate to place the far-field boundary at $\zeta_{max} \to \infty$. Moreover, the truncation errors in the solutions using the transformed variables are different from those obtained with the untransformed variables. While constant increments in the $(N,S)$ coordinates correspond to $(\eta,\zeta)$ increments that become progressively larger as $\eta,\zeta$ increase, the present transformation, Eq. (10), with a $(51 \times 51)$ grid, is such that, for $\eta,\zeta \leq 5.0$, the $(\eta,\zeta)$ increments are less than 0.4. Recalling

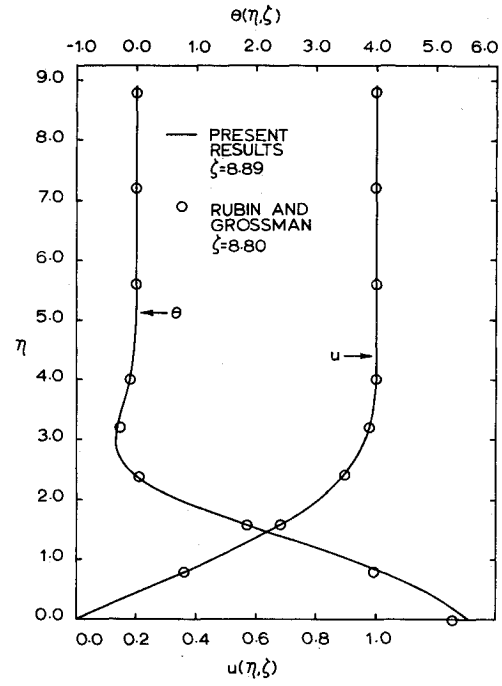


**Fig. 2 Comparison for finite region calculations—streamwise velocity and vorticity.**

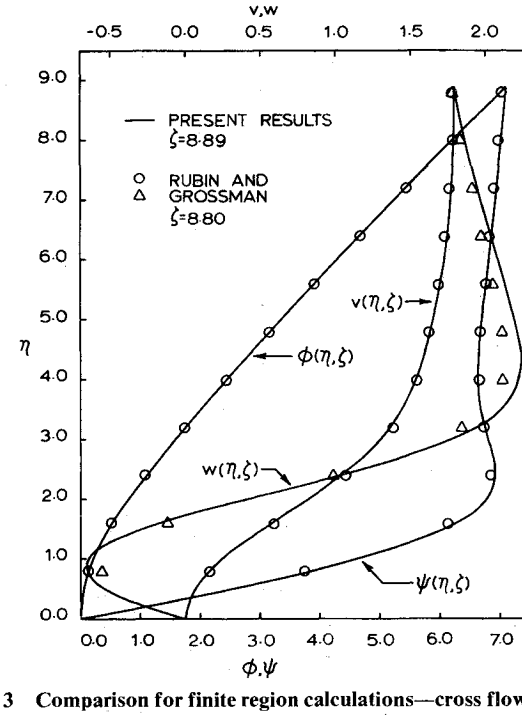


**Fig. 3 Comparison for finite region calculations—cross flow velocity parameters.**

that the finite region solution in terms of $(\eta,\zeta)$ was obtained with constant steps $\Delta\eta = \Delta\zeta = 0.4$, it appears that the 10% discrepency in $\bar{w}(\eta,\eta)$ occurring near $\eta = 4.0$ may not be attributed to the local truncation errors caused by the $N,S$ transformations. In fact, the transformation used permits better resolution of the problem in the interior of the corner layer.

Also, contrary to the finite corner results, is the appearance of small negative $v$ velocity in the very interior of the corner, when the infinite corner region is solved. These are more clearly seen in Fig. 6 where the direction of the arrows represents the local secondary flow direction given by $\tan^{-1}(v/w)$. The secondary flow streamlines may be easily traced from these results, if desired. It is important to note that the arrows do not represent the magnitude of the local velocity, so

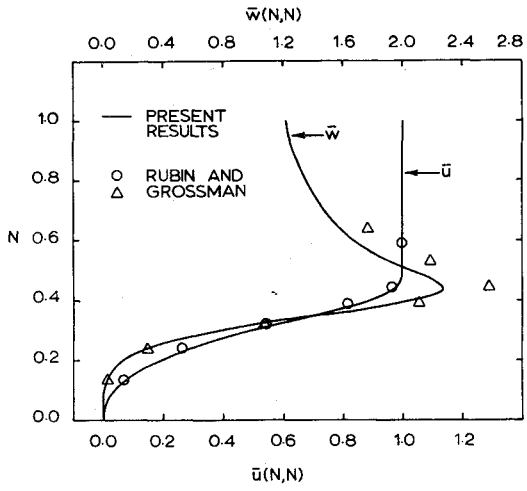


**Fig. 4 Velocities along symmetry line of infinite corner.**

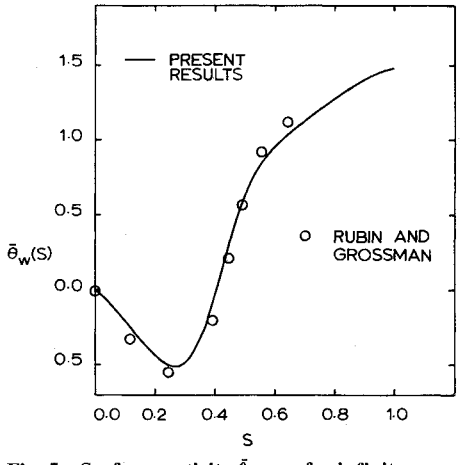


**Fig. 5 Surface vorticity $\bar{\theta}_{WALL}$ for infinite corner.**

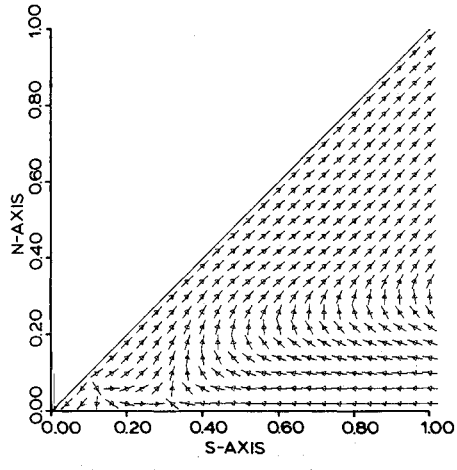


**Fig. 6 Secondary flow direction.**

that arrows issuing away from or converging towards a certain point, do not imply the presence of a source or a sink. As seen from this figure for secondary flow, there is a region of inflow towards the corner near the plate surface and an outward flow parallel to the symmetry line away from the corner. In spite of the simple geometry involved, the structure of the secondary flow in the corner layer is remarkably complex. The qualitative sketch of the secondary flow presented by Rubin and Grossman[4] bears considerable similarity to the present results, except in the very interior of the corner, where the results are markedly different.

Before presenting these results here, efforts were made to confirm the presence of these negative $v$ velocities. It was noticed that the initial values of the problem were such that $v$ was negative in the inner region of the corner. It could be possible that, although the final solution satisfied the prescribed convergence criterion, changes could still be occurring in the third or fourth figure after the decimal, so that these small negative $v$ velocities, of the order of $10^{-2}$, could change sign and become small positive quantities. Therefore, results were also obtained with the problem initialization changed such that $v$ was everywhere positive initially. Nevertheless, the final solution still showed small negative $v$ in the inner corner region, for $\eta, \zeta$ less than about 0.4.

The presence of negative $v$ in the inner corner region may be the first indication of a possible closed vortex in the secondary flow. However, no closed secondary flow vortex is seen in the present results, although the secondary flow streamlines in the inner region are considerably more curved than indicated in the earlier results of Rubin and Grossman. Closed secondary vortices have been reported in studies of turbulent corner flow. The mechanism for the origin of these closed vortices has been discussed clearly in the noteworthy study of Eichelbrenner and Preston,[8] but no closed vortices have been obtained for the laminar secondary flow in the corner. However, the recent analysis of Tokuda[5] for the Stokes slow-flow region, embedded in the corner layer, has established the presence of a series of viscous eddies in the Stokes region. This is a local phenomenon and would have no appreciable effect on the streamwise velocity in the general corner layer solution, but could have an observable influence on the cross flow velocities. Being a local phenomenon, the Stokes eddies are confined to very small $\eta$ and $\zeta$. If a numerical solution for the entire corner layer is to reproduce these viscous eddies, a highly refined mesh would be required in the very interior of the corner The present mesh is certainly finer than that used earlier in the finite region solutions, so that it places some points in the Stokes region, but not fine enough to reproduce the closed vortex. This may be a partial answer for the nature

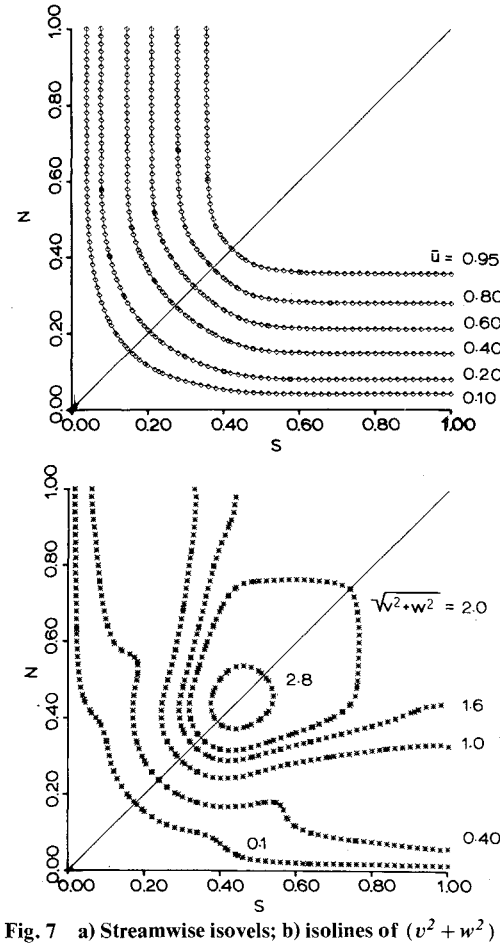


**Fig. 7 a) Streamwise isovels; b) isolines of $(v^2 + w^2)^{1/2}$.**

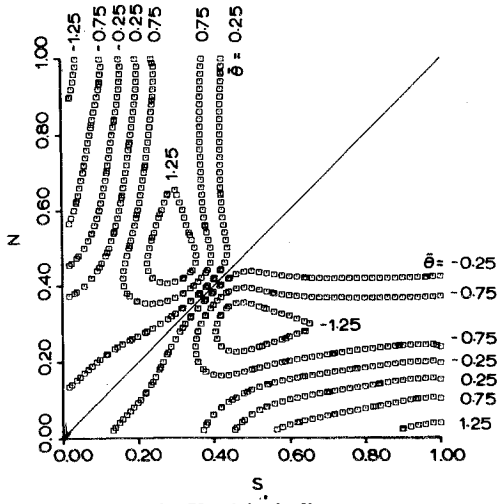


Fig. 8 Vorticity isolines.

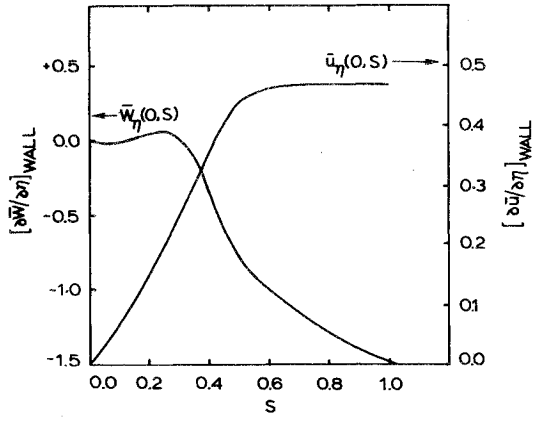


Fig. 9 Wall shear stress functions for infinite corner.

of the cross flow observed in Fig. 6. Somewhat similar observations have been reported by Roache[9] for the driven cavity problem where a finer mesh was needed in order to locate the closed secondary vortices near the lower corners of the cavity. One may also need to ascertain whether the streamwise similarity conjectured for the corner layer flow would be satisfied in the Stokes flow region.

The isovels for the streamwise velocity $\bar{u}$ are shown in Fig. 7a which also provides a good idea about the extent of the viscous region for the corner flow geometry. The bulge predicted by the experiments of Zamir and Young[10] is not observed in the present results. Since $v$ and $w$ reflect as $w$ and $v$, respectively, across the symmetry line $\eta=\zeta$, plotting $v$ or $w$ contours in the entire corner would present a misleading picture about the symmetry of the flow about the line $\eta=\zeta$. Therefore, the contour plots of the total secondary velocity $(v^2+w^2)^{1/2}$ convey more significance as shown in Fig. 7b. Contour plots of the vorticity function $\bar{\theta}$ are presented in Fig. 8. Finally, the shear stress $u_\eta$ on the plate surface $\eta=0$ is plotted as a function of distance along the plate. As seen in Fig. 9, the surface shear is zero at the corner line due to the symmetry of the flow along the corner bisector, and increases monotonically to approach its asymptotic value corresponding to two-dimensional Blasius flow. If the extent of the corner layer in the $\zeta-$direction is defined to be the distance where the wall shear $u_\eta(0,\zeta)$ reaches 0.99 of its asymptotic 2-D value, then Fig. 9 shows that the corner layer extends to about two to three times the Blasius boundary-layer thickness. The cross flow shear stress parameter $w_\eta(0,\zeta)$ is also shown in this figure; the repeated zeros are an indication of the reversals of the $w$-profiles in the corner. Although the present analysis provides the solution for the infinite corner problem, the results should be interpreted with care when $\eta$ or $\zeta$ or both $\eta,\zeta$ are large, because the coordinates used are not optimal for this problem.[11] The two-dimensional analog of this situation is the classical problem of boundary-layer flow over a semi-infinite flat plate in Cartesian coordinates or similarity variables obtained therefrom. The solution outside the viscous region departs from the true solution as the transverse similarity coordinte becomes large. If the flat plate problem is solved in parabolic coordinates which are optimal for this flow problem, then a uniformly valid boundary-layer solution is obtained. It must be noted that, inside the corner layer region, the results are independent of the coordinate system employed and, hence, accurate and reliable.

## IV. Conclusions

The streamwise flow in the infinite region of an axial corner has been analyzed. The results provide details of the flow structure for the corner problem and reproduce the earlier finite corner region solutions for the streamwise velocity and the vorticity function. The secondary flow pattern obtained shows some differences from the finite region solution, but the differences are not too surprising if one takes into consideration the Stokes flow solution of Tokuda[5] for the corner problem.

The analysis and numerical method developed for the unbounded corner flow circumvents the need for higher-order asymptotic solutions for this problem with algebraic asymptotic behavior. The determination of higher-order asymptotic solutions requires considerable algebra even for the incompressible flow over the simple geometry considered here. This difficulty becomes especially severe in the analysis of general compressible corner region flow. The present approach alleviates this difficulty by providing a unified analysis for the entire infinite corner region. The method developed makes it now possible to solve the general compressible corner flow problem for which only the far-field boundary conditions have been recently determined.[12] The basic numerical method should also be useful in solving other flow problems of the boundary-region type, e.g., the flow on the leeside of conical bodies at angle of attack, where a boundary-layer analysis becomes invalid on account of large secondary flows.

## Reference

[1] Rubin, S. G., "Incompressible Flow Along a Corner," *Journal of Fluid Mechanics*, Vol. 26, Part 1, Sept. 1966, pp. 97-110.

[2] Stewartson, K., "Viscous Flow Past a Quarter-Infinite Plate," *Journal of the Aerospace Sciences*, Vol. 28, Jan. 1961, pp. 1-10.

[3] Pal, A. and Rubin, S. G., "Asymptotic Features of the Viscous Flow Along a Corner," *Quarterly of Applied Mathematics*, Vol. 29, April 1971, pp. 91-108.

[4] Rubin, S. G. and Grossman, B., "Viscous Flow Along a Corner: Numerical Solution of the Corner Layer Equations," *Quarterly of Applied Mathematics*, Vol. 29, July 1971, pp. 169-186.

[5] Tokuda, N., "Viscous Flow Near a Corner in Three Dimensions," *Journal of Fluid Mechanics*, Vol. 53, Part 1, May 1972, pp. 129-148.

[6] Ghia, K. N. and Davis, R. T., "Corner Layer Flow: Optimization of Numerical Method of Solution," *International Journal of Computers and Fluids*, Vol. 2, March 1974, pp. 17-34.

[7] Sills, J. A., "Transformations for Infinite Regions and Their Applications to Flow Problems," *AIAA Journal*, Vol. 7, Jan. 1969, pp. 117-123.

[8] Eichelbrenner, E. A. and Preston, J. H., "On the Role of Secondary Flow in Turbulent Boundary Layers in Corners (and Salients)," *Journal De Mecanique*, Vol. 10, March 1971, pp. 91-112.

[9] Roache, P. J., "Finite-Difference Methods for the Steady-State Navier-Stokes Equations," *Lecture Notes in Physics*, Vol. 18, Springer-Verlag, Berling, 1973.

[10] Zamir, M and Young, A. D., "Experimental Investigation of the Boundary Layer in a Streamwise Corner," *Aeronautical Quarterly*, Vol. 21, Nov. 1970, pp. 313-339.

[11] Davis, R. T. and Ghia, U., "The Use of Optimal Coordinates in the Solution of Viscous Flow Problems," Aerospace Engineering Rept. No. AFL 73-8-4, Aug. 1973, University of Cincinnati, Cincinnati, Ohio.

[12] Ghia, K. N. and Davis, R. T., "A Study of Compressible Potential and Asymptotic Viscous Flows for Corner Region," *AIAA Journal*, Vol. 12, March 1974, pp. 355-359.